

# A parametric study and modal analysis of an acoustic black hole on a beam

K. Hook<sup>1</sup>, J. Cheer<sup>1</sup>, S. Daley<sup>1</sup>

<sup>1</sup> The Institute of Sound and Vibration Research, Faculty of Engineering and the Environment,  
The University of Southampton, Southampton, United Kingdom  
e-mail: [k.hook@soton.ac.uk](mailto:k.hook@soton.ac.uk)

## Abstract

Acoustic black holes are structural features that have a varying thickness profile, and provide a potential lightweight damping solution for flexural vibrations. In practical applications, the length of an acoustic black hole will be constrained by the available space and the minimum tip height will be limited by both the manufacturing capabilities and strength requirements. Therefore, the power law of the taper is often the critical design parameter. In this paper, a parametric study of an acoustic black hole termination on a beam is presented with practical constraints on the length and tip height. The reflection coefficient of the acoustic black hole has been calculated for a range of power laws and it has been shown that, for a fixed power law, the reflection coefficient varies over frequency and exhibits bands of high and low reflection. These bands can be related to modes of the acoustic black hole. In addition, it has been found that an optimum power law exists for minimising the broadband average reflection coefficient for each acoustic black hole configuration.

## 1 Introduction

The acoustic black hole effect, as described by Mironov in 1988 [1], is a phenomenon that occurs when a beam or plate is tapered to a point, over a distance equal to or larger than the acoustic wavelength. Figure

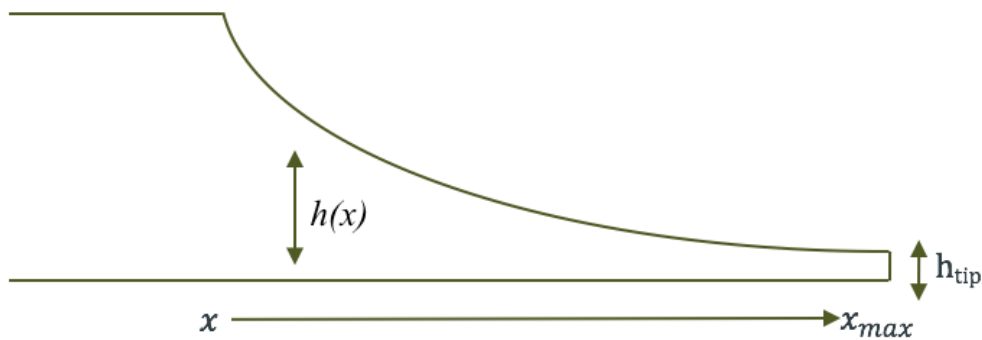


Figure 1: A diagram of an acoustic black hole taper.

1 shows an example of an acoustic black hole, seen as the tapering of the beam to a point via a power law curve. The behaviour of such an acoustic black hole can be explained by considering flexural vibrations travelling down a tapered Euler-Bernoulli beam. As the vibrations propagate towards the tip, their velocity is reduced following the relationship

$$c_b = \sqrt[4]{\frac{Eh^2(x)\omega^2}{12\rho}} \quad (1)$$

where  $E$  is the Young's modulus of the beam material,  $h(x) = \varepsilon x^\mu + h_{tip}$  is the height function of the beam,  $\omega$  is the angular frequency of the vibrations,  $\rho$  is the density of the beam material and  $\nu$  is the poisson ratio [2,3]. For a tapered semi-infinite plate, the same equation may be used by the inclusion of the poisson ratio term:  $1/(1 - \nu^2)$  [4]. It can be seen, from equation 1, that the wave speed in a tapered beam is proportional to the square root of the beam height. It follows that, as the height function tends to zero, the velocity of a propagating wave converges to zero. Hence, the propagating wave will theoretically never reach the tip of the taper and therefore will not reflect back out of the taper. In reality, a perfect and infinite tapered beam cannot be manufactured and the structural integrity of the acoustic black hole is questionable for very thin tip heights. It has previously been shown that the acoustic black hole effect is negligible for practical tip heights, but that improvements could be made to the effectiveness by applying thin viscoelastic damping layers to either one or both sides of the taper, which results in a significant reduction in the reflection coefficient from the acoustic black hole [5–7]. It is clear that there is a tradeoff between practicality and performance in the design of acoustic black holes.

Over time, there has been an increase in the amount of literature modelling more practically dimensioned acoustic black holes. This has coincided with an increase in experimental studies, used to validate the models, which are limited by manufacturing restrictions on the tip height and length of the taper. The thickness tends to range from about a 10mm beam or plate height down to a 0.25mm tip height. The taper lengths are usually up to 10cm long and the power law of the taper tends to be between 2 and 4. Damping layers, applied to the acoustic black hole taper, have usually been thin but theory predicts that the thickness of the damping layer can be up to six times the thickness of the base layer before the increase in loss factor diminishes [8,9].

So far, work has been done that examines the influence of the tip height and power law on the modal density of an acoustic black hole on a beam [10]. It has been shown that a smaller tip height significantly increases the modal density of an acoustic black hole. Higher power laws cause a slight increase in modal density. The modal density of the acoustic black hole on a beam was not found to be related to the modal density of a uniform beam [10]. In addition to this, band gaps have been observed in acoustic black holes. For an acoustic black hole cell, the mode shapes of the bounding frequencies of the band gaps have been matched to the mode shapes of the resonant frequencies [11]. These band gaps have also been shown to vary in range and frequency when the power law of the acoustic black hole taper is changed, and when the tip height is changed. The optimum thickness of damping has been investigated with the use of a laser as both an excitation and measurement device, which also allowed visualisation of wave propagation and small imperfections in the structure [7].

This paper will investigate the potential link between the reflection coefficient of an acoustic black hole, the band gaps mentioned in [11] and the different controllable parameters of an acoustic black hole. In this paper, a finite element model of a lightly damped acoustic black hole on a beam is presented and used to investigate the design tradeoff between the geometric parameters. The reflection coefficient for frequency dependant parameter sweeps and broadband frequency parameter tradeoffs is then shown and there is a discussion of the findings. A link between the modes of an acoustic black hole and the power law of the taper is presented alongside a discussion about optimising the power law for practical application. Finally, the conclusions of this work are presented.

## 2 The finite element model of an ABH on a beam

In order to carry out a parametric study of the acoustic black hole, a finite element model of an acoustic black hole on the end of a long beam has been developed. The beam was assigned a width of 4cm, a length of 3m and a height of 1cm. The acoustic black hole shared the same width and starting height as the beam. The beam and taper were both assumed to be constructed from aluminium and a small amount of isotropic damping ( $\eta = 0.07$ ) was applied to the acoustic black hole taper in addition to the natural damping properties of aluminium. It should be noted that isotropic damping does not have frequency dependant characteristics and is therefore not the most accurate representation of a practical, thinly applied, damping layer. However,

isotropic damping was considered to be suitable for this investigation since it is the profile of the taper that is being investigated rather than the damping layer itself. The initial conditions of the acoustic black hole were set to stationary and the boundary conditions of all the edges were set to free. A point force of 10N was applied to the end of the beam furthest from the acoustic black hole. Finally, the two dimensional model was meshed using an edge element mesh. To determine the necessary mesh size, a convergence study was carried out which determined the number of elements required per wavelength for both the beam section and the acoustic black hole section. Although it is possible to mesh the acoustic black hole with a spatially varying element size, for simplicity the acoustic black hole was meshed in a uniform manner and the reference wavelength was taken from the tip so that there would be *at least* the required number of elements per wavelength to obtain accurate results. An example of the difference in mesh size for the

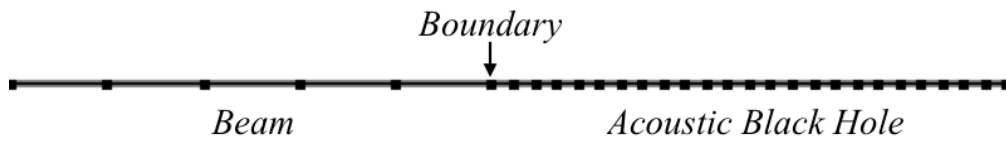


Figure 2: The meshing difference between the beam, on the left, and the acoustic black hole, on the right.

acoustic black hole and beam section is shown in Figure 2, where the difference in mesh resolution for the beam and taper sections is clear. The displacement of the acoustic black hole calculated by the model when it is being excited at 2kHz is shown in Figure 3. Note that, because the displacement has been magnified

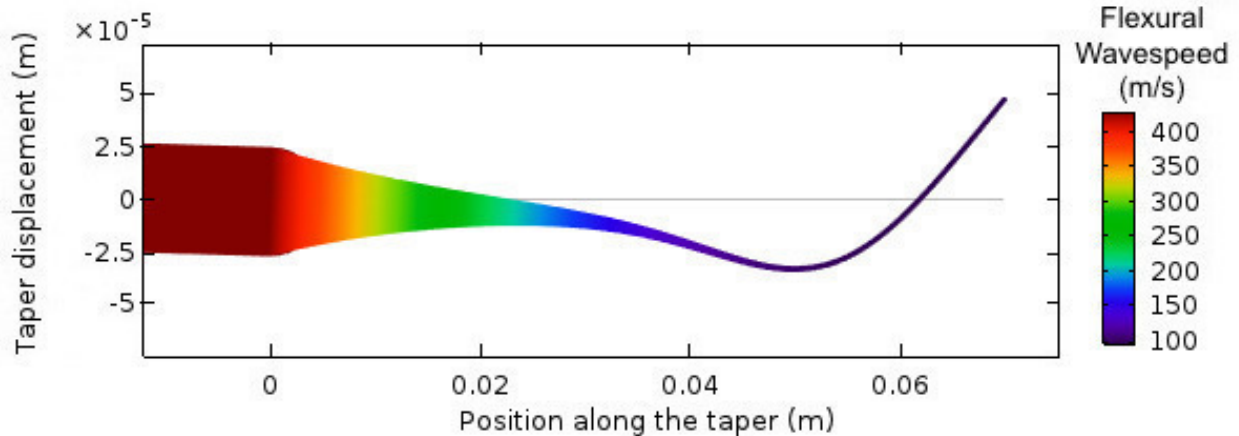


Figure 3: The position along the taper plotted against the displacement of the taper for an excitation of 10N at 2000Hz. The flexural wave speed is shown as a colour scale.

for clarity, the taper height in Figure 3 is not to scale. The flexural wave speed has also been included to demonstrate the acoustic black hole effect (ie the slowing of the wave speed) occurring towards the tip. For reference, the dimensions of the model can be found in the default column of Table 1 in Section 3.

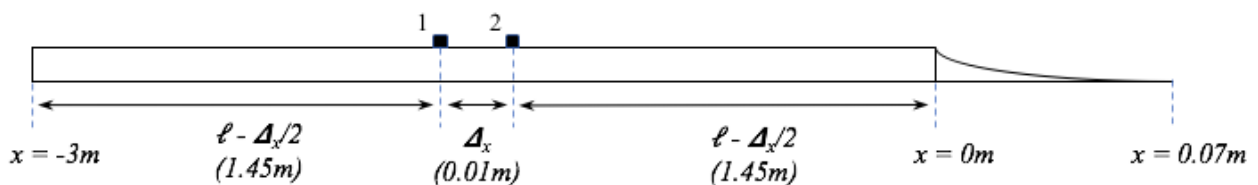


Figure 4: The evaluation points used on the beam for measurement of the acoustic black hole reflection coefficient.

Two evaluation points were added midway along the beam section, shown in Figure 4, at  $x = -1.55\text{m}$  and  $x = -1.45\text{m}$  to allow calculation of the reflection coefficient. The transverse acceleration of the beam was evaluated at these two points. Based on the sensor separation, an upper frequency limit can be defined as

$$f_{max} = \frac{c_b}{2\Delta_x} \quad (2)$$

where  $\Delta_x$  is the separation between the two sensor points and  $f_{max}$  is the upper frequency limit [12]. The influence of near field effects can be assumed negligible (max contribution  $\approx 0.04$ ) if the sensor array is at least half a wavelength away from the primary source and any significant changes in the structure (ie the ABH). Therefore, a lower frequency limit can be defined as

$$f_{min} = \frac{1}{8\left(\ell - \frac{\Delta_x}{2}\right)^2} \quad (3)$$

where  $f_{min}$  is the lower frequency limit and  $\ell$  is the distance from the sensor array to the primary source [12]. The evaluation points were 1.45m from either the input force or the discontinuity in the beam formed by the taper and therefore near field effects could be neglected at frequencies above 0.06Hz. Therefore, assuming these limits are fulfilled, the wave amplitudes of the positive and negatively travelling propagating waves can be calculated as

$$A = \frac{i(a_1 e^{\frac{ik_B \Delta_x}{2}} - a_2 e^{-\frac{ik_B \Delta_x}{2}})}{2\omega^2 \sin(k_B \Delta_x)} \quad (4)$$

$$B = \frac{i(a_2 e^{\frac{ik_B \Delta_x}{2}} - a_1 e^{-\frac{ik_B \Delta_x}{2}})}{2\omega^2 \sin(k_B \Delta_x)} \quad (5)$$

where  $a$  is the measured acceleration at the data acquisition points 1 and 2 (shown in Figure 4),  $A$  and  $B$  are the complex amplitudes of the positive and negative travelling waves respectively,  $\omega$  is the angular frequency and  $k_B$  is the bending wavenumber, calculated as

$$k_B = \sqrt[4]{\frac{\rho_s S}{EI_z}} \sqrt{\omega} \quad (6)$$

where  $\rho_s$  is the cross-sectional density,  $S$  is the cross-sectional area,  $E$  is the Young's modulus of the material and  $I_z$  is the cross-sectional moment of inertia. The reflection coefficient can then be calculated by taking the ratio of the reflected to the incident wave amplitudes,

$$R = \left| \frac{B}{A} \right|. \quad (7)$$

This technique has commonly been used for the calculation of the reflection coefficient for acoustic samples [12–15] and also for vibrational samples in acoustic black holes [16].

### 3 A parametric study and modal analysis of acoustic black holes

To investigate the effect that design parameters have on the acoustic black hole performance, a parametric study has been performed and the reflection coefficient has been evaluated as a function of the different parameters. The three parameters of interest: tip height, taper power and taper length were swept over the ranges specified in Table 1. The parameter ranges were chosen with a consideration of manufacturing restrictions. The acoustic black hole taper has been defined using the geometrical expression

$$h(x) = \varepsilon[(l - x)/l]^\mu + h_{tip} \quad (8)$$

Parameters		
Parameter	Range being swept	Default if not being swept
Power law ( $\mu$ )	2 to 10	4
Taper length ( $l$ )	50mm to 500mm	70mm
Tip height ( $h_{tip}$ )	0.5mm to 10mm	0.5mm
Frequency ( $f$ )	100Hz to 10000Hz	-
Beam height ( $h_{beam}$ )	-	10mm
ABH / Beam width	-	40mm
ABH isotropic damping ( $\eta$ )	-	0.07
Structure material	-	Aluminium

Table 1: The range over which each parameter was swept in the finite element model and the default values for the structural parameters.

where  $\varepsilon = h_{beam} - h_{tip}$ . This expression Provides an exponentially decreasing taper, whilst allowing separate control over the taper length, tip height and power law, allowing each parameter to be changed independently.

The frequency was swept on a logarithmic scale from 100Hz to 10000Hz using the expression

$$f_{range} = 10^{\log_{10}(f_{min}) : 1/490 : \log_{10}(f_{max})} \quad (9)$$

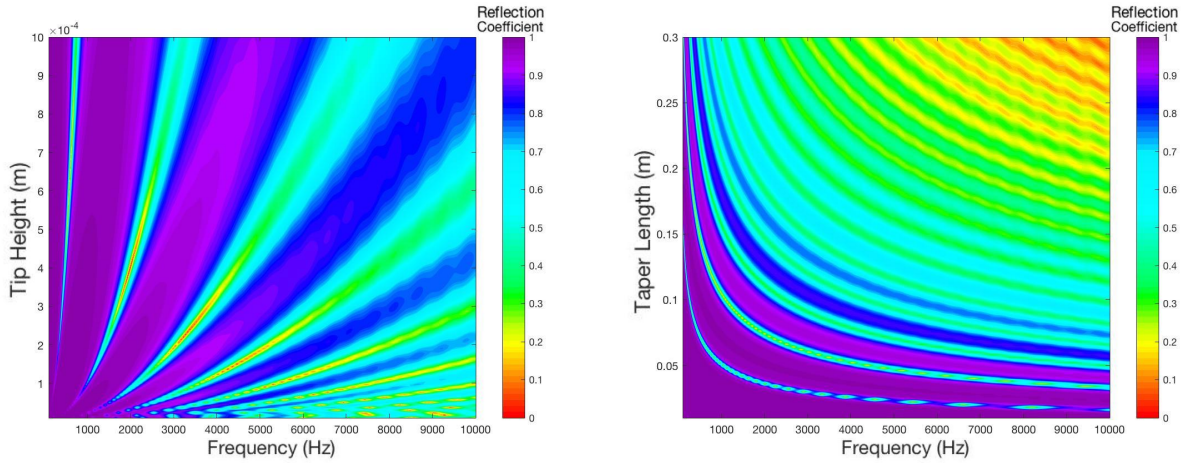
in order to account for the smaller bandwidths of low frequency resonances by increasing the frequency step density at the low end.

It is important to note that due to the low damping factor used, the reflection from the acoustic black hole is generally relatively high. This paper aims to provide insight into how the behaviour of an acoustic black hole can be related to its modal characteristics and this behaviour is clearer for low damping factors and, therefore, a low damping factor has been used to provide physical insight into the behaviour.

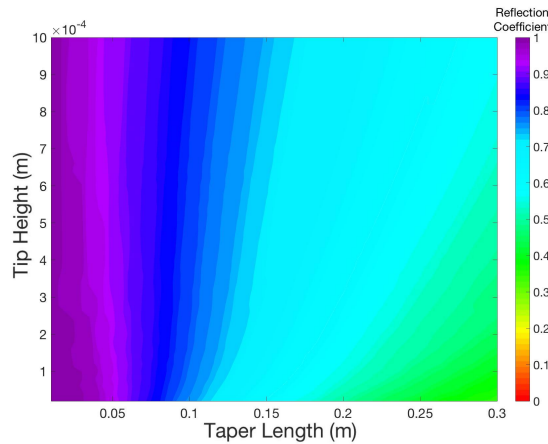
Figure 5a shows how the reflection coefficient of the acoustic black hole varies with different tip heights over a frequency range of 100Hz to 10000Hz. The results show that for smaller tip heights, the frequency bands of low reflection decrease in width but increase in density so that there is, in general, a lower amount of reflection from the tip. Also, at higher frequencies the bands of low reflection are wider and therefore there is less reflection from the tip at higher frequencies. These results demonstrate that there is periodic spectral variation in the reflection coefficient of an acoustic black hole that is dependant on the tip height.

Figure 5b shows how the reflection coefficient of the acoustic black hole varies with taper length over a frequency range of 100Hz to 10000Hz. The results show that at any frequency, a longer acoustic black hole taper produces a lower reflection coefficient. At higher frequencies, there is less reflection for any taper length. Considering the small damping coefficient used, a longer taper length appears to produce very low reflection, which indicates that the acoustic black hole effect is working well. These results are also consistent with the literature and demonstrate that the performance of an acoustic black hole is better for longer taper lengths and at higher frequencies. These results also show the spectral variation in the reflection coefficient of an acoustic black hole.

Figure 5c shows how the broadband average of the reflection coefficient varies with the taper length and tip height of an acoustic black hole. These results show that on average, the reflection decreases for longer tapers and for smaller tip heights. At a taper length shorter than 0.05m, the practical range of tip heights that were examined appeared to have no effect on the average broadband reflection coefficient. As the taper length increases above 0.05m, the tip height of the acoustic black hole has more influence on the average broadband reflection coefficient and a smaller tip height produces lower reflection. For any tip height examined, the average broadband reflection coefficient decreases as the taper length increases. There was a 0.12 average difference in the reflection coefficient between the smallest and largest tip height and, in contrast to this,



(a) Tip height plotted against frequency for an acoustic black hole with a taper length of 70mm and a power law of 4. (b) Taper length plotted against frequency for an acoustic black hole with a tip height of 0.5mm and a power law of 4.



(c) The tradeoff between the tip height and the taper length of an acoustic black hole with a power law of 4.

Figure 5: The reflection coefficient, plotted on a scale of 0 to 1, as a function of frequency and a parameter (5a, 5b), and as a tradeoff between two parameters for a broadband frequency average (5c).

there was a 0.49 average difference in the reflection coefficient between the shortest and longest taper length.

Figure 6 shows how the reflection coefficient of an acoustic black hole varies with the taper power law over a frequency range of 100Hz to 10000Hz. These results show that as the power law of the taper increases for a single frequency, a particular range of power law values produces a low reflection coefficient. At higher frequencies, there are more power law values that produce a low reflection coefficient for a specific frequency. For any given power, at higher frequencies the bands of low reflection are wider. At low power laws, these bands become very wide and this results in a cut-on frequency for each power law, above which the acoustic black hole produces low reflection.

The white dotted lines shown in Figure 6 show how the frequencies of the first five modes of the acoustic black hole cell vary with the power law. The acoustic black hole cell is the acoustic black hole without the beam section (i.e. just the taper). From the results shown in Figure 6, it can be seen that the modes of the acoustic black hole occur at the same frequencies as the minima in the reflection coefficient. It can also be seen that as the power law increases, the modal frequencies decrease. The power law could, therefore, be used to tune the modal frequencies and thus the frequency bands of low reflection. In practice, this could be

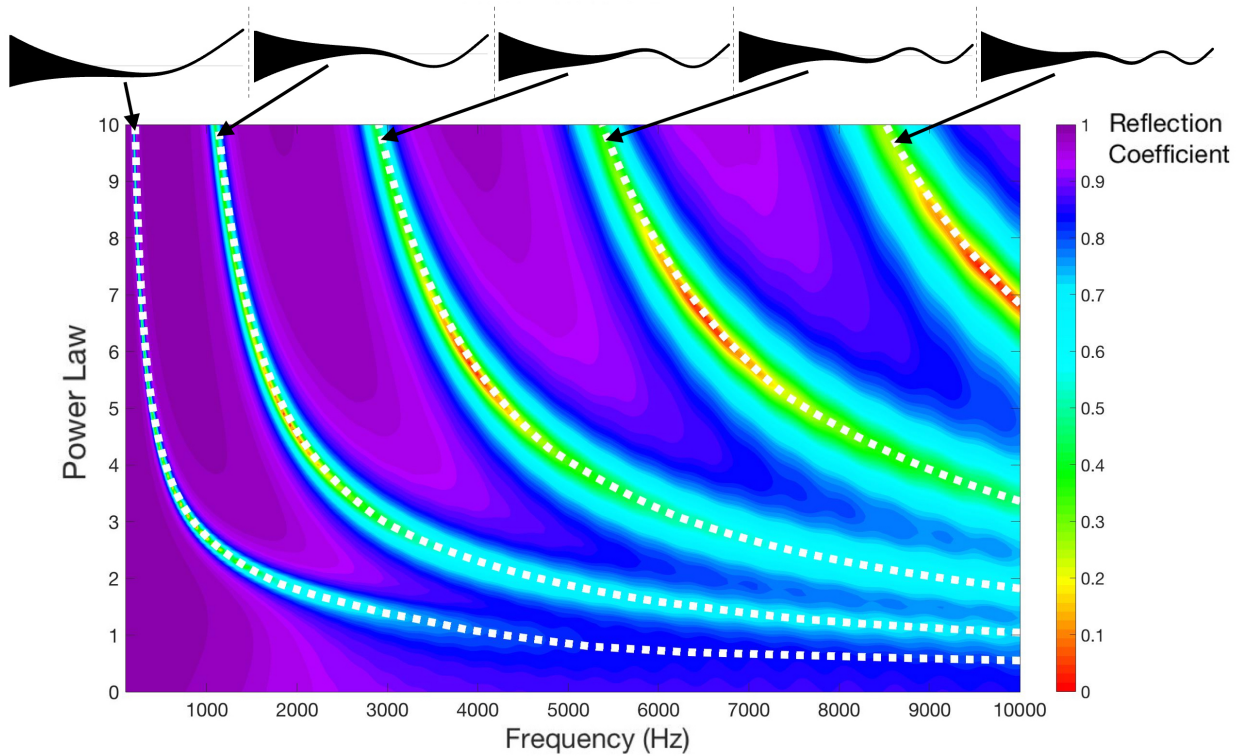


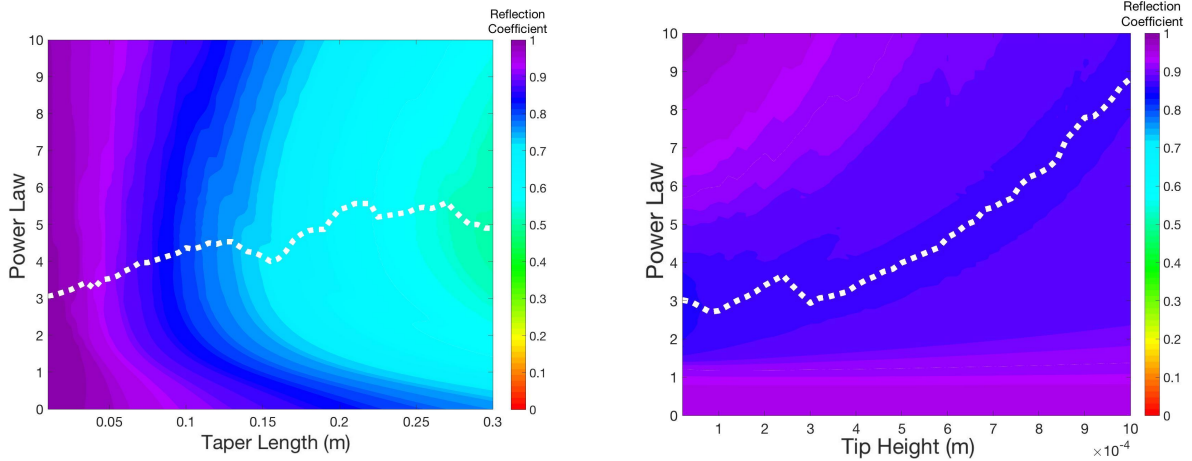
Figure 6: The power law of the taper plotted against frequency for an acoustic black hole with a tip height of 0.5mm and a taper length of 70mm. The reflection coefficient is represented by a colour scale from 0 to 1. An overlay of the first 5 modal frequencies for different power laws, and their shapes, are shown by the white dotted lines.

used to tune the bands of low reflection to the resonant frequencies of a structure.

Figure 7a shows the tradeoff between the power law of the acoustic black hole and the taper length. These results show that there is an optimum power law for the average broadband performance of an acoustic black hole at a specific taper length. For a longer taper length, the optimum power law is slightly higher than for a shorter taper length. The optimum power law at each taper length is shown by a dotted white line. This confirms that the power law, a key controllable parameter, can be optimised for a specific taper length. Figure 7b shows the tradeoff between the power law of the acoustic black hole and the tip height. These results show that there is an optimum power law that can be used to achieve a minimum average broadband reflection at a specific tip length. For a larger tip height, the optimum power law is higher than for a smaller tip height. The optimum power law at each tip height is shown by a dotted white line. The power law can therefore be optimised for a specific tip height. As seen earlier in Figure 5c, over a practical range with a small amount of damping, increasing the taper length appears to have more influence on the reflection coefficient than decreasing the tip height. However, both Figures 7a and 7b show that for an acoustic black hole of practical dimensions (shown as the default values in Table 1), the optimum power law is approximately 4. Optimising and tailoring the power law can be useful, for example, when the working environment of an acoustic black hole is restricted geometrically. In such a scenario, the power law can still be used to optimise the broadband reflection coefficient for the particular length and tip height of the acoustic black hole.

## 4 Conclusions

This paper presents an extended study of how the controllable parameters influence the reflection coefficient and broadband frequency average reflection coefficient of an acoustic black hole on a beam. An investigation



(a) The tradeoff between the power law of the taper and the taper length for an acoustic black hole with a tip height of 0.5mm. (b) The tradeoff between the power law of the taper and the tip height of the acoustic black hole. The taper length was set at 70mm.

Figure 7: The broadband frequency average reflection coefficient, plotted on a scale of 0 to 1, as a tradeoff between the power law and the taper length (7a) and the power law and the tip height (7b). For both tradeoffs, the optimum power law for a minimum broadband reflection coefficient has been marked on with a dotted white line.

was carried out to determine how the power law of an acoustic black hole can be used as a key design parameter for acoustic black holes with practical dimensions and a modal analysis was performed to observe the modal band gaps in the reflection coefficient and their dependence on the power law of the taper.

It has been shown that an acoustic black hole has a higher performance if designed with a longer taper length and smaller tip height. The influence of these two parameters on the reflection coefficient of the acoustic black hole has been shown for a range of sweep values and a tradeoff between the two parameters has also been shown. The results are as predicted for individual cases in the literature: a longer taper and smaller tip height produces a better energy absorption and therefore a lower reflection coefficient. However, when designing acoustic black holes for practical applications, these two parameters are likely to be constrained, leaving the power law of the acoustic black hole taper as the key controllable parameter.

The reflection coefficient of an acoustic black hole has been shown to exhibit spectral variation over a range of power law values, present as frequency bands of low reflection. Raising the power law has been shown to shift the bands of low reflection down in frequency and also increase the width of the bands. The modal analysis has shown that the frequencies of an acoustic black hole's modes match the frequencies of the bands of low reflection coefficient. The frequency of the modes has been shown to change with the power law of the taper, making the power law a key controllable parameter when designing acoustic black holes, especially for practical applications where the length and tip height may be constrained. A tradeoff plot between the tip height and the taper length of an acoustic black hole has shown that, for the practical parameter range investigated, increasing the taper length had more influence on the reflection coefficient than decreasing the tip height. Tradeoff plots between the power law and both tip height and taper length have both shown that there exists an optimum power law for the geometry of an acoustic black hole that results in the lowest broadband reflection coefficient. For the practically dimensioned acoustic black hole tested this was found to be around 4. When utilised in a practical application, an acoustic black hole might be used to damp particular frequency bands or provide an overall attenuation in a restricted space. Both of these cases can be optimised by changing the power law of the acoustic black hole taper.



## Acknowledgements

This work was supported by an EPSRC iCASE studentship.

The authors acknowledge the use of the IRIDIS High Performance Computing Facility, and associated support services at the University of Southampton, in the completion of this work.

## References

- [1] M.A. Mironov *Propagation of a flexural wave in a plate whose thickness decreases smoothly to zero in a finite interval*, Soviet Physics: Acoustics, Vol. 34, No. 3, American Institute of Physics (1988), pp. 318-319.
- [2] F.J. Fahy and J.G. Walker *Fundamentals of Noise and Vibration*, Spon Press (1998).
- [3] L. Cremer, M. Heckl and B.A.T. Petersson *Structure Borne Sound*, 3rd edition, Springer (2005).
- [4] A.N. Norris *Flexural waves on narrow plates*, The Journal of the Acoustical Society of America, Vol. 113, No. 5, Acoustical Society of America (2003), pp. 2647-2658.
- [5] V.V. Krylov and F.J.B.S. Tilman *Acoustic 'black holes' for flexural waves as effective vibration dampers*, Journal of Sound and Vibration, Vol. 274, No. 3-5, Elsevier (2004), pp. 605-619.
- [6] L. Zhao *Passive vibration control based on embedded acoustic black holes*, Journal of Vibration and Acoustics, Vol. 138, No. 4, The American Society of Mechanical Engineers (2016), pp. 1-6.
- [7] H. Ji, J. Qiu, J. Luo and L. Cheng *Investigations on flexural wave propagation and attenuation in a modified one-dimensional acoustic black hole using a laser excitation technique*, Mechanical systems and signal processing, Vol. 104, Elsevier (2018), pp. 19-35.
- [8] E.M. Kerwin Jr. *Damping of plate flexural vibrations by means of viscoelastic laminae*, ASME Annual Meeting Structural Damping, New York (1959), pp. 49-87.
- [9] M.R. Shepherd, P.A. Feutado and S.C. Conlon *Multi-objective optimization of acoustic black hole vibration absorbers*, The Journal of the Acoustical Society of America, Vol. 140, No. 3, Acoustical Society of America (2016), pp. 227-230.
- [10] V. Denis, A. Pelat, F. Gautier and B. Elie *Modal overlap factor of a beam with an acoustic black hole termination*, Journal of Sound and Vibration, Vol. 333, No. 12, Elsevier (2014), pp. 2475-2488.
- [11] L. Tang and L. Cheng *Broadband locally resonant band gaps in periodic beam structures with embedded acoustic black holes*, Journal of Applied Physics, Vol. 121, No. 19, AIP Publishing (2017), pp. 1-9.
- [12] C.R. Halkyard and B.R. Mace *Feedforward adaptive control of flexural vibration in a beam using wave amplitudes*, Journal of Sound and Vibration, Vol. 254, No. 1, Elsevier (2002), pp. 117-141.
- [13] S.J. Elliott, C.R. Fuller and P.A. Nelson *Active Control of Vibration*, Academic Press (1996)
- [14] B.H. Song and J.S. Bolton *A transfer-matrix approach for estimating the characteristic impedance and wave numbers of limp and rigid porous materials*, Journal of Sound and Vibration, Vol. 107, No. 3, Elsevier (2000), pp. 1131-1152.
- [15] C.R. Halkyard and B.R. Mace *Structural intensity in beams - waves, transducer systems and the conditioning problem*, Journal of Sound and Vibration, Vol. 185, No. 2, Elsevier (1995), pp. 279-298.

- [16] V. Denis, F. Gautier, A. Pelat, and J. Poittevin *Measurement and modelling of the reflection coefficient of an acoustic black hole termination*, Journal of Sound and Vibration, Vol. 349, Elsevier (2015), pp. 67-79.